

Selective recovery and separation of rare earth elements by organophosphorus modified MIL-101(Cr)

Kavun, Vitalii; van der Veen, Monique A.; Repo, Eveliina

DOI

[10.1016/j.micromeso.2020.110747](https://doi.org/10.1016/j.micromeso.2020.110747)

Publication date

2020

Document Version

Final published version

Published in

Microporous and Mesoporous Materials

Citation (APA)

Kavun, V., van der Veen, M. A., & Repo, E. (2020). Selective recovery and separation of rare earth elements by organophosphorus modified MIL-101(Cr). *Microporous and Mesoporous Materials*, 312, Article 110747. <https://doi.org/10.1016/j.micromeso.2020.110747>

Important note

To cite this publication, please use the final published version (if applicable). Please check the document version above.

Copyright

Other than for strictly personal use, it is not permitted to download, forward or distribute the text or part of it, without the consent of the author(s) and/or copyright holder(s), unless the work is under an open content license such as Creative Commons.

Takedown policy

Please contact us and provide details if you believe this document breaches copyrights. We will remove access to the work immediately and investigate your claim.

Green Open Access added to TU Delft Institutional Repository

'You share, we take care!' – Taverne project

<https://www.openaccess.nl/en/you-share-we-take-care>

Otherwise as indicated in the copyright section: the publisher is the copyright holder of this work and the author uses the Dutch legislation to make this work public.



Selective recovery and separation of rare earth elements by organophosphorus modified MIL-101(Cr)

Vitalii Kavun^{a,*}, Monique A. van der Veen^b, Eveliina Repo^a

^a Department of Separation Science, LUT University, Yliopistonkatu 34, 53850, Lappeenranta, Finland

^b Catalysis Engineering, Department of Chemical Engineering, Delft University of Technology, Van der Maasweg 9, 2629 HZ, Delft, the Netherlands

ARTICLE INFO

Keywords:

Metal-organic frameworks
Rare earth elements
Chemical stability
Adsorption modelling
Erbium

ABSTRACT

Development of state-of-the-art selective adsorbent materials for recovery of rare earth elements (REEs) is essential for their sustainable usage. In this study, a metal-organic framework (MOF), MIL-101(Cr), was synthesized and post-synthetically modified with optimised loading of the organophosphorus compounds tributyl phosphate (TBP), bis(2-ethylhexyl) hydrogen phosphate (D2EHPA, HDEHP) and bis(2,4,4-trimethylpentyl) phosphinic acid (Cyanex®-272). The materials were characterized and their adsorption efficiency towards Nd³⁺, Gd³⁺ and Er³⁺ from aqueous solutions was investigated. The MOF derivatives demonstrated an increase in adsorption capacity for Er³⁺ at optimal pH 5.5 in the order of MIL-101-T50 (37.2 mg g⁻¹) < MIL-101-C50 (48.9 mg g⁻¹) < MIL-101-H50 (57.5 mg g⁻¹). The exceptional selectivity of the materials for Er³⁺ against transition metal ions was over 90%, and up to 95% in the mixtures with rare earth ions. MIL-101-C50 and MIL-101-H50 demonstrated better chemical stability than MIL-101-T50 over 3 adsorption–desorption cycles. The adsorption mechanism was described by the formation of coordinative complexes between the functional groups of modifiers and Er³⁺ ions.

1. Introduction

Rare earth elements (REEs), as critical materials [1], are essential in fields such as the production of high-tech electronic devices and the development of green technologies. To enable a move away from high-grade ores processing with its high energy costs, projected supply shortages and access issues, it is necessary to develop more sustainable methods for recovery and concentration of REEs. Recycling of secondary resources, such as electronic waste, has been attracting considerable interest [2,3] as many of these resources contain valuable elements, for instance, light (La, Nd and Gd) and heavy (Dy, Ho and Er) REEs [4,5]. Moreover, such recycling contributes towards circular economy.

Electronic waste usually contains a small amount (ppm level) of REEs [6] available for further extraction and concentration. The applied hydrometallurgy techniques [2,7], chemical precipitation [8], extraction processes [9,10] and ion exchange [11] possess drawbacks, such as high operating costs, hazardous acidic environments, non-selectivity, and high losses of REEs, especially at low initial concentrations. Clearly, there is a lack of green and cost-efficient methods for effective REE recovery [12].

Adsorption is a feasible alternative for the recovery and separation of

rare earth metals due to its environmentally-friendly characteristics, low cost, tuneable selectivity towards REEs, and applicability at low initial concentrations [13]. In recent years, porous adsorbent materials, such as zeolites, silica gel, activated carbon, ion-exchange resins, have been extensively studied and widely applied in a commercial use for broad-ranging wastewater treatments, including recovery of rare earth metals. However, the efficiency of a porous material is highly dependent on its and the adsorbate's nature as well as the aqueous media conditions. For example, the final uptake of Nd³⁺ varies from 7.3 to 232 mg of Nd³⁺ per gram of a material [14]. Although adsorption has many advantages, the reusability of the adsorbents and their selectivity towards REEs in the presence of other metals may be uncertain and differ depending on process conditions.

Metal-organic frameworks (MOFs), a relatively new class of porous adsorbent materials, are constructed from an inorganic part of metal clusters interconnected by an organic part of rigid linkers, resulting in a highly crystalline structure with a large specific surface area, and adjustable volume and porosity [15,16]. These compounds have been successfully used in such applications as heterogeneous catalysis, storage and separation of gases [17], electrochemistry [18] and photocatalysis [19,20]. Their application as adsorbent materials for various

* Corresponding author.

E-mail address: vitalii.kavun@lut.fi (V. Kavun).

<https://doi.org/10.1016/j.micromeso.2020.110747>

Received 29 April 2020; Received in revised form 18 September 2020; Accepted 2 November 2020

Available online 4 November 2020

1387-1811/© 2020 Elsevier Inc. All rights reserved.

compounds, including heavy metal ions, has been studied to some extent [21,22], but only a limited number of publications have investigated adsorption of REEs. Thus, the full potential of this type of porous materials for recovery of REEs is not fully known.

Although MOFs have favourable characteristics, their structural stability in aqueous solutions remains a challenge. MIL-101(Cr) has been found to have remarkable stability during long-term exposure to acidic and alkaline solutions, H₂O₂ and air [23], and it could thus be considered an appropriate candidate for REE recovery. However, the pristine MIL-101(Cr) showed a weak affinity towards REEs, while a post-synthetic modification by various functional groups enhanced the adsorption capacity and selectivity, making it a promising material compared to traditional adsorbents [24].

As typical Lewis acids, REEs have strong affinity to Lewis bases, for instance, phosphorous or various oxygen-based functional groups [25]. Organophosphorus compounds such as TBP, HDEHP and Cyanex-272 (Table S1) are well-known selective acid extractants (Lewis bases) for REEs [26–28]. Several studies have reported the possible functionalization of different substrates [29–32] by organophosphorus extractants. In the study by Shu et al. [32], a HDEHP modified silica-based adsorbent demonstrated relatively high adsorption capacities of 39.6 and 51.4 mg g⁻¹ for Ce³⁺ and Gd³⁺, respectively. In other work, synthesized zirconium organophosphates and phosphorous acid-modified mesoporous SBA-15 showed high uptake of Eu⁺³ (60 mg g⁻¹) [33] and Gd³⁺ (200 mg g⁻¹) [34], respectively. Moreover, it has also been demonstrated that a combination of –POH and –COOH groups on the surface of zirconium-based coordination polymers [35] and MIL-101(Cr)-PMIDA [24] can result in an adsorption capacity for Gd³⁺ of higher than 90 mg g⁻¹.

While some studies were carried out on efficient recovery of REEs using MOFs, the challenge experienced by separation between light and heavy REEs over the past decades remains unresolved [36]. Moreover, there is no studies in which a high separation efficiency between HREEs and LREEs has been achieved. Therefore, in this work, the possibility to develop a stable and selective adsorbent by combining attractive characteristics of MIL-101 and extraction ability of the modifiers was considered.

Furthermore, to the best of the authors' knowledge, the functionalization of MOFs, specifically MIL-101(Cr), by organophosphorus extractants for recovery of REEs has hitherto not been investigated. In this study, a post-synthetic modification of MIL-101(Cr) was carried out using Cyanex-272, HDEHP and TBP. The synthesized materials were characterized and subsequently tested in aqueous solutions of REEs (Nd³⁺, Gd³⁺ and Er³⁺) to investigate adsorption behaviour, reusability and separation performance for transition metal ions and REEs.

2. Experimental section

2.1. Materials and material characterization methods

A list of materials and material characterization methods used in the experimental studies is given in Sections S1 and S2, respectively.

2.2. Synthesis of adsorbent materials

2.2.1. Synthesis of MIL-101

Hydrothermal synthesis was carried out in accordance with the reported procedure [37] with slight modification: nitric acid was utilized as a mineralizing agent instead of hydrofluoric acid. The synthesis details are provided in Section S3.

2.2.2. Preparation of mixtures of Cyanex-272, HDEHP and TBP

For each modifier, Cyanex-272, HDEHP and TBP, a specified amount of mmol (3.5, 7, 15, 35 and 70) was weighed and added to toluene to obtain the desired mass fraction of the compound in the solvent (5, 10, 20, 50 and 100 wt%, respectively).

2.2.3. Synthesis of MIL-101-Cx, MIL-101-Hx and MIL-101-Tx

First, the synthesized MIL-101 (2.18 g) was treated at 140 °C in a vacuum oven for 12 h. Afterwards, the activated MIL-101 was suspended at a ratio of 37 mg of MOF for each of the solutions prepared in Section 2.2.2. The mixtures were stirred at 100 °C for 6 h. Then, each functionalized product was separated from the mixture by vacuum filtration using PTFE membrane filters and subsequently washed with ethanol and dried in an oven at 85 °C for 12 h.

2.3. Adsorption experiments with REEs

Generally, 10 mg of adsorbent was mixed with 10 mL of a solution and agitated at 320 rpm at 21 °C for 24 h to reach equilibrium. After filtration by 0.45 µm polypropylene syringe filter, the concentration of the initial solution and filtrate were analysed by ICP-MS.

The effect of pH was studied using Er³⁺ at a concentration of 100 ppm with adjusted pH from 1.0 to 6.0. pH adjustment was carried out by adding appropriate amounts of dilute solutions of 0.1 M HCl or NaOH.

Data for adsorption equilibrium isotherms were collected from adsorption experiments with concentrations of Er³⁺ in the range of 10–500 ppm at pH 5.5, which were prepared from an initial 1000 ppm solution.

The kinetic studies were performed using initial 100 and 150 ppm Er³⁺ solutions with a contact time from 5 min to 24 h at pH 5.5.

After each experiment, the equilibrium capacity (q_e , mg g⁻¹) of the adsorbents was calculated using Eq. (1):

$$q_e = \frac{(C_i - C_e) \times V}{m} \quad (1)$$

where C_i and C_e (mg L⁻¹) are initial and equilibrium concentrations of the analysed element, respectively, and V (L) is the volume of the solution and m (g) is the mass of the adsorbent.

The affinity of the synthesized materials towards Nd³⁺, Gd³⁺, and Er³⁺ ions was estimated based on the distribution coefficient value, K_d (mL g⁻¹) and calculated using Eq. (2):

$$K_d = \frac{(C_i - C_e)}{C_e} \times \frac{V}{m} \quad (2)$$

where V is the volume of the solution given in mL.

Adsorption selectivity of the adsorbents towards Er³⁺ from a solution containing transition metal ions and lighter REEs was investigated. Mixtures of Er³⁺, Cu²⁺, Co²⁺, Ni²⁺ and Zn²⁺ at a concentration of 50 ppm each and Nd³⁺, Gd³⁺ and Er³⁺ at a concentration of 100 ppm each were prepared and pH was adjusted to 5.5. The selectivity (%) was calculated as the amount of adsorbed Er³⁺ ions divided by the total amount of adsorbed ions multiplied by 100.

Reusability tests were conducted at several steps. Modified adsorbents were mixed and agitated with a 100 ppm solution of Er³⁺ at pH 5.5. After 24 h, the adsorbent material was separated from the solution by vacuum filtration and dried under vacuum conditions. Then, the adsorbents were regenerated by agitation in 1 M HNO₃ for 3 h. The adsorption and desorption cycles were repeated 3 times.

3. Results and discussions

For MOFs, such as MIL-100(Fe), MIL-101(Cr) and HKUST-1, where the structure allows coordinatively unsaturated sites (CUS), removal of solvent molecules is essential to obtain CUS suitable for post-synthetic modification [15]. Therefore, an extensive washing procedure followed by vacuum heating of the prepared MIL-101(Cr) was performed to generate open metal sites for coordinative interaction with modifier agents [38–41]. Then, the activated green powder was functionalized with organophosphorus compounds (Fig. 1) at different ligand/toluene ratios.

The products were designated MIL-101-Cxwt%, MIL-101-Hxwt%

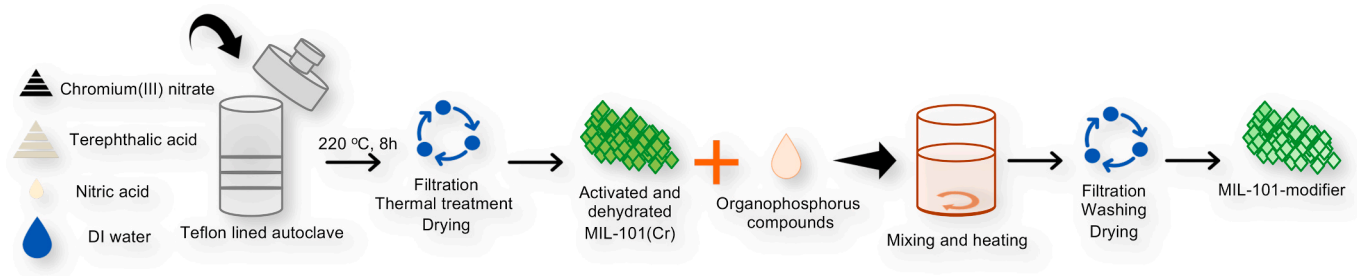


Fig. 1. Schematic representation of synthesis of MIL-101(Cr) and its modification with organophosphorus ligands.

and MIL-101-Txwt%, where x refers to the weight percentage of added component to toluene and C, H and T are attributed to Cyanex-272, HDEHP and TBP ligands, respectively. The synthesized series of adsorbent derivatives were further tested to assess the effect of dosage of phosphorous compounds on the adsorption capacity for Er^{3+} .

As can be seen from Table S2, the adsorption capacities, q_e , increased in the order of MIL-101-Txwt% < MIL-101-Cxwt% < MIL-101-Hxwt%, while the pristine MIL-101 demonstrated weak affinity towards Er^{3+} . In general, the metal uptake increased as the dosage of an extractant increased. However, no significant difference in q_e values between 50 and 100 wt% loading was observed. Therefore, further studies were

performed with 50 wt% mixtures and the final materials were named MIL-101-C50, MIL-101-H50 and MIL-101-T50.

3.1. Characterization of prepared materials

3.1.1. PXRD patterns

The crystalline structure of as-prepared MIL-101 and its derivatives was confirmed by PXRD (Fig. 2a and Figure S1). The diffraction peaks in the patterns are consistent with those reported previously [37,38], indicating that grafting of the functional groups on the surface of adsorbent does not affect the general crystallinity even at the highest

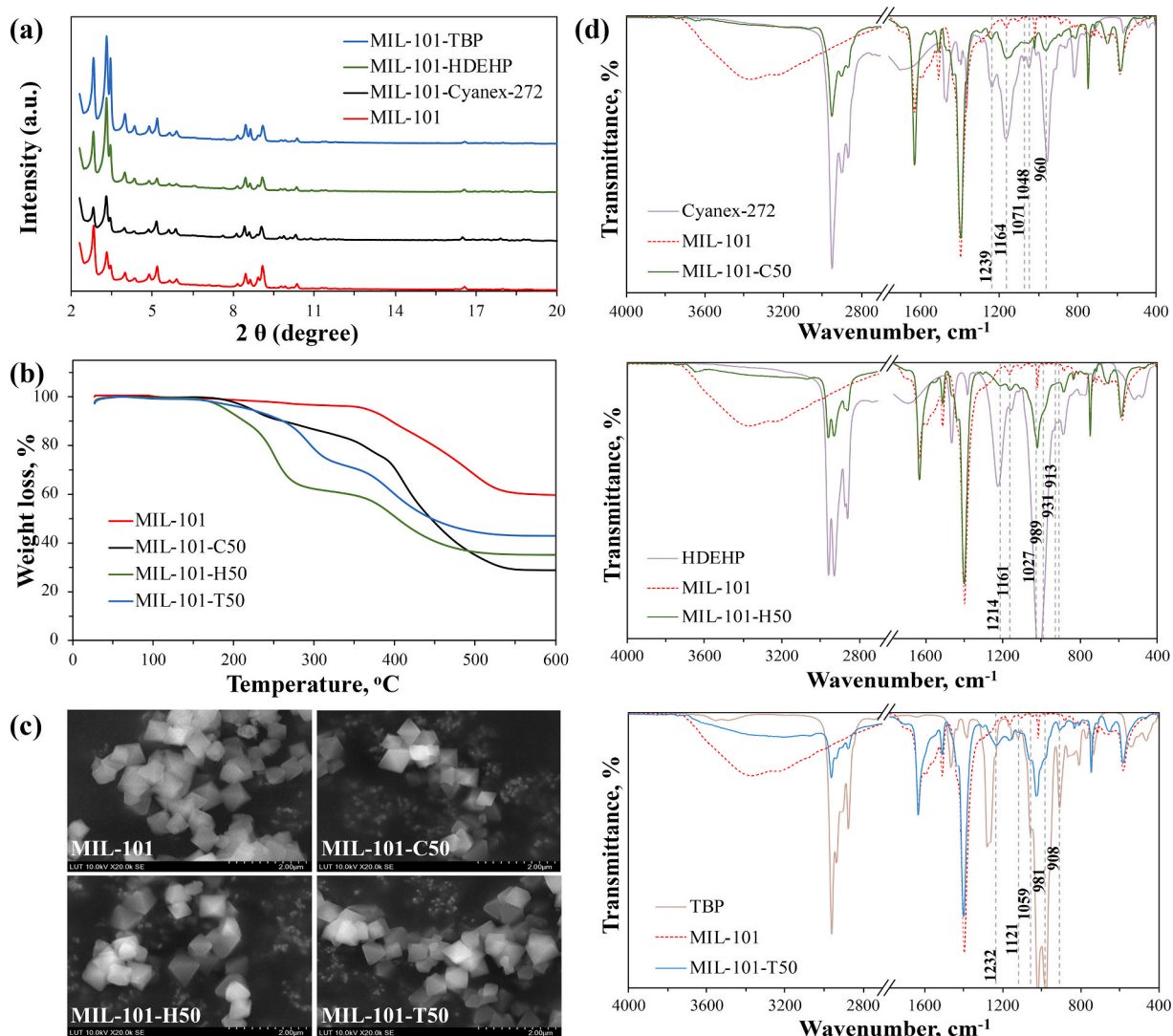


Fig. 2. PXRD patterns (a), TGA curves (b), SEM images (c) and FTIR spectra (d) of pristine and functionalized MIL-101.

loading of modifiers.

3.1.2. SEM

SEM images of the synthesized materials (Fig. 2c and Figure S2) confirmed the octahedral morphology of the crystals and uniform distribution of particle size (≈ 700 nm) [42]. Modification of MIL-101 with organophosphorus compounds did not lead to aggregation, change of particle size or appearance of crystalline defects, which is in line with the PXRD data (Fig. 2a).

3.1.3. TGA

Thermogravimetric analysis of the pristine MIL-101 (Fig. 2b) showed the first weight loss between 40 and 100 °C, which is related to release of physically adsorbed water [38]. The adsorbent was relatively stable until 350 °C. However, further increase in temperature led to decomposition of the bdc^{2-} ligand, followed by degradation of the MOF structure [43]. Closer inspection of Fig. 2b shows that the first significant weight loss of the modified samples starts at 200 °C, associated with decomposition of the grafted organophosphorus compounds [29], and continues up to 340 °C. MIL-101-C50 showed continuing degradation within the studied temperature range, making it a challenging task to determine the adsorbed amount. The calculated loading of a modifier on the surface of MIL-101 corresponds to 1.15 mmol g^{-1} of HDEHP (3.63 CUS per HDEHP molecule) and 1.03 mmol g^{-1} of TBP (4.08 CUS per TBP molecule), demonstrating high extractant loading compared to the theoretical maximum of 1.47 anchored molecules per 1 g of MIL-101(Cr) [44].

3.1.4. BET analysis

Summary from nitrogen sorption measurements of the synthesized materials is provided in Table 1 and Table S3. MIL-101 shows expected high specific surface area ($3341 \text{ m}^2 \text{ g}^{-1}$) with high pore volume ($1.8 \text{ cm}^3 \text{ g}^{-1}$). These results are attributed to replacement of hydrofluoric acid with nitric acid during the synthesis of MIL-101, which is in line with previous studies [40,42,45]. Moreover, the additional effect of increased porosity and a greater number of available active sites for incorporation of modifiers on the surface of the adsorbent was also observed. The analysis of the functionalized MOFs shows that successive increase of the modifier ligand dosage leads to a lower surface area (Table S3) ascribed for the partial filling or blockage of pores by adsorbed molecules of extractant.

Detailed analysis of MIL-101 indicates a small step observable at $p/p_0 = 0.2$ of MIL-101 attributed to the different fillings of the MOF cages by N_2 [38,46]. Furthermore, MIL-101-H50 and MIL-101-T50 demonstrate Type-I adsorption isotherms [47] (Figure S3) with detectable decrease in micropore volume (Table 1).

Possible changes in the structure and morphological properties of MIL-101-C50 were, however, not detected from XRD data and SEM images. The observable divergence of adsorption and desorption branches at low-pressure ($p/p_0 < 0.42$) of N_2 sorption isotherm may indicate specific interactions between nitrogen and alkyl chains [47–50] of grafted Cyanex-272. However, the complex interactions prevented reliable estimates of the pore size and volume.

3.1.5. FTIR spectra

FTIR spectra of the organophosphorus compounds, and MIL-101 and

its modifications are shown in Fig. 2d and Figure S4. Intense peaks in the range of $2961\text{--}2860 \text{ cm}^{-1}$ can be seen for all materials, which are assigned to stretching vibrations of aliphatic $-\text{CH}_2$ and $-\text{CH}_3$ methyl groups of organic chains of organophosphorus extractants. The $\text{P}=\text{O}$ stretching vibration was presented by signals at 1232 and 1121 cm^{-1} (TBP), 1214 and 1161 cm^{-1} (HDEHP), and 1239 and 1164 cm^{-1} (Cyanex-272). The additional peaks within the range of $1060\text{--}980 \text{ cm}^{-1}$ after modification by HDEHP and TBP were ascribed to $\text{P}\text{--}\text{O}\text{--}\text{C}$ asymmetric stretching vibration. The bands at 1071 and 1048 cm^{-1} of MIL-101-C50 can be attributed to symmetric $\text{P}\text{--}\text{O}$ stretching. At lower frequencies, all phosphorous-grafted adsorbents showed a sharp peak in the range of $960\text{--}908 \text{ cm}^{-1}$, which can be ascribed to $\text{P}\text{--}\text{O}$ stretching [50–53]. The presence of these new peaks in the structure provides strong evidence for successful functionalization of MIL-101. Moreover, a clear trend of increasing intensity of specific phosphorus vibrations of MIL-101 derivatives was observed as a function of increase in extractant concentration (Figure S4), indicating more available functional groups of Cyanex-272, HDEHP and TBP for adsorption of specific ions. This observation is consistent with the rising trend of metal uptake of Er^{3+} when the dosage of extractant (wt%) in the solution increases (Table S2).

3.2. Effect of solution pH on Er^{3+} adsorption

Selection of an appropriate range of solution pH is of particular importance and has a significant impact on adsorption of REEs. To prevent the appearance of unfavourable species, the sorption studies of Er^{3+} were conducted in pH range from 1 to 6 [54].

Fig. 3a clearly indicates that the adsorption of Er^{3+} is pH dependent for all samples. The pristine MIL-101 shows negligible adsorption of Er^{3+} throughout the studied pH range. In contrast, metal uptake by the modified samples occurs already at pH 1 and reaches a plateau at $\text{pH} > 4$. However, MIL-101-T50 shows slightly different behaviour, demonstrating the highest adsorption capacity of 29.3 mg g^{-1} already from pH 2.

The extraction process using TBP as an organic phase is followed by a solvation mechanism, assuming the formation of complexes with anions in the solution, metal cations and TBP molecules [55]. The ion-exchange mechanism ascribed to Cyanex-272 and HDEHP consists of exchanging hydrogen atoms with REEs $^{3+}$ [56]. It can be seen from Fig. 3a that an increase in pH enhances the adsorption capacities of MIL-101-C50 and MIL-101-H50, indicating that the functional groups of HDEHP and Cyanex-272 can be deprotonated and exchanged with Er^{3+} ions [50]. The pK_a values of HDEHP and Cyanex-272 in pure water are reported to be 2.75 and 3.73 [57–59], respectively, signifying stronger acidity of HDEHP than Cyanex-272. Therefore, a possible explanation for the higher adsorption capacity of MIL-101-H50 could be the higher available surface area and better proton donation capability (i.e. lower pK_a).

Under acidic conditions or at elevated temperatures, TBP molecules can be degraded to dibutyl or monobutyl phosphates by cleaving one or two $\text{C}\text{--}\text{O}$ bonds (dealkylation), respectively. Therefore, possible dealkylation of grafted TBP molecules may create an adsorption site for positively charged ions. The low Er^{3+} uptake at pH 1 of MIL-101-T50 can be ascribed to protonation of the functional groups, which causes electrostatic repulsion between the positively charged adsorption sites and Er^{3+} ions. Nevertheless, the adsorption behaviour of the material at pH

Table 1
Physical properties of MIL-101 and the modified materials.

Sample	BET surface area ($\text{m}^2 \text{ g}^{-1}$)	Pore volume ($\text{cm}^3 \text{ g}^{-1}$)	Average pore diameter (nm)	t-Plot micropore volume ($\text{cm}^3 \text{ g}^{-1}$)
MIL-101	3341	1.80	2.27	0.40
MIL-101-H50	972	0.47	2.66	0.27
MIL-101-T50	1206	0.57	2.77	0.20

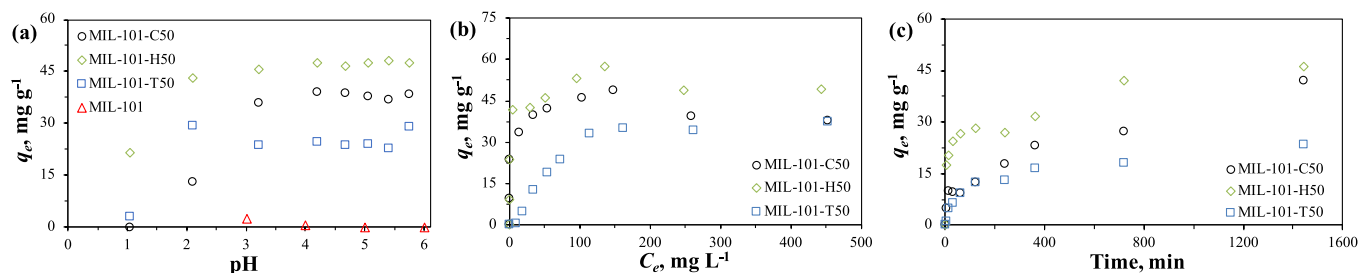


Fig. 3. Effect of pH on Er^{3+} adsorption efficiency (a), adsorption isotherms at pH 5.5 (b) and effect of contact time on Er^{3+} adsorption at pH 5.5 of 100 ppm solution (c) on the functionalized MIL-101.

> 2 is similar to that of TBP modified carbon nanotubes reported previously [60].

Possible risks of grafting on coordinatively unsaturated chromium sites have been reported in several studies [24,43,61]. Disruption of the bonds between metal active sites of MIL-101 and the grafted functional groups can occur because of preferable coordination with water molecules. In this study, however, XRD and FTIR analyses after the pH experiments confirmed the preservation of functional groups and the framework stability (Figure S5 and Figure S6). Additionally, the concentration of Cr and P in the supernatants was measured before and after adsorption to monitor possible leaching of the elements from the substrates (Table S4). In the case of MIL-101-H50 and MIL-101-C50, the ICP-MS results showed up to 90% less leached Cr over the operating pH (i.e. pH 1–6) than with MIL-101-T50 and pristine MIL-101, indicating that the higher stability of these functionalized adsorbents is caused by excluding possible interactions between water or other guest molecules and Cr(III) sites of MIL-101(Cr) [16].

In general, the observable phosphorous leaching increases in the order of MIL-101-H50 < MIL-101-C50 < MIL-101-T50 with an average 0.1, 0.5 and 5 $\mu\text{mol g}^{-1}$, respectively. Moreover, the concentration of phosphorous of MIL-101-T50 at pH 1 was almost double the concentration for the rest of the pH range. The high phosphorous leaching might be attributed to the partial detachment of functional groups of MIL-101-T50 due to the relatively high solubility of TBP in acidic conditions [62] and replacement of functional groups by water molecules. In addition to the high adsorption capacity for Er^{3+} at pH 5.5, it should be noted that almost no leaching of Cr as well as the lowest phosphorus content was found at this pH, providing further justification for the selection of pH 5.5 for subsequent adsorption experiments.

3.3. Adsorption isotherms

The adsorption isotherms were obtained by determining the amount of Er^{3+} adsorbed by the functionalized MIL-101 materials (q_e , mg g^{-1}) plotted against the concentration of Er^{3+} in supernatant (C_e , mg L^{-1}) at the equilibrium state.

The maximum equilibrium adsorption capacities, q_{max} , of MIL-101-C50 and MIL-101-H50 were experimentally found at concentration of 200 mg L^{-1} and reached 48.91 and 57.47 mg g^{-1} , respectively, while for MIL-101-T50 the highest value was observed only at 500 mg L^{-1} with $q_{max} = 37.21 \text{ mg g}^{-1}$ (Fig. 3b). It is interesting to note that the adsorption capacity of the HDEHP modified sample is higher than that of the Cyanex-272 functionalized materials, which contrasts with the final metal uptake of magnetite nanoparticles functionalized with the same modifiers in a previous study [29] and might be related to differences in the nature of the substrates.

To determine the type of sorption mechanism between the Er^{3+} ions and adsorption sites of the MOF adsorbents, different sorption models (described in Section S5) were fitted to the equilibrium data (Figure S7). The isotherm parameters and corresponding correlation coefficients are summarized in Table S5. As can be seen, the slope of the isotherms of all studied samples indicates an energetically favourable adsorption

process. Fitting of the experimental data for MIL-101-C50 and MIL-101-H50 did not show a reasonable difference between the applied models but suggested prevalent heterogeneity of the surface of the adsorbents ($1/n < 1$). Furthermore, the q_e values of MIL-101-C50 and MIL-101-H50 decrease by about 23% and 15%, respectively, as the concentration of Er^{3+} solution increases from 200 ppm to 500 ppm.

In contrast, the sorption process of MIL-101-T50 was appropriately fitted with the Sips model [63], with a correlation coefficient of $R^2 > 0.99$, indicating heterogeneity of the active sites on the surface and exponential distribution of their energies at low concentrations. Thus, the slightly S-shaped curve at the beginning of the sorption isotherm may be related to low affinity towards Er^{3+} at initial steps, which subsequently changes to the saturation region at higher concentrations [64, 65].

3.4. Adsorption kinetics

To estimate the kinetics of Er^{3+} adsorption and determine the rate-controlling process, sorption experiments were carried out at contact time ranging from 5 min to 24 h. As can be seen from Fig. 3c and Figure S8, the equilibrium plateau is reached after 24 h for all three samples. Moreover, within the first 6 h, half of the maximum saturation capacity is attained for MIL-101-C50 and MIL-101-T50, while for MIL-101-H50, the same result is reached within 3 h, indicating faster kinetics at initial stages.

To investigate the sorption process, different kinetic models [66] were applied to the experimental data (Figure S9 and Figure S10). A detailed description of the models is given in Section S6 and the constants of the final models and R^2 values are summarized in Table S6. It can be seen that none of the models was able to be perfectly fitted to the kinetic data of MIL-101-C50 and MIL-101-H50. The complexity of the adsorption process and hardly accessible adsorption sites are limiting factors, signifying that the mechanisms of the models in each case could not be considered as the only rate controlling steps. In contrast, MIL-101-T50 could be fitted well with the Weber and Morris model at both low and high concentrations of Er^{3+} (Table S6), suggesting that pore diffusion is a predominant mechanism for the rate-controlling step. This finding is in agreement with previously reported work on TBP-modified carbon nanotubes [60].

3.5. Selectivity tests

In practical applications, favourable selectivity of the adsorbent towards specific species is of paramount importance. Leaching solutions of electronic waste, such as motherboards and hard drive magnets, consist of various multivalent ions (e.g. Co^{2+} , Cu^{2+} , Ni^{2+} and Zn^{2+}) which can affect the metal uptake by competing for free adsorption sites on the adsorbent surface.

As can be observed from Fig. 4a, all three modified samples demonstrated strong selectivity (>90%) towards Er^{3+} in the presence of transition ions. Selectivity targeting the Er^{3+} ion increased in the order of MIL-101-C50 < MIL-101-H50 < MIL-101-T50. MIL-101-T50 showed

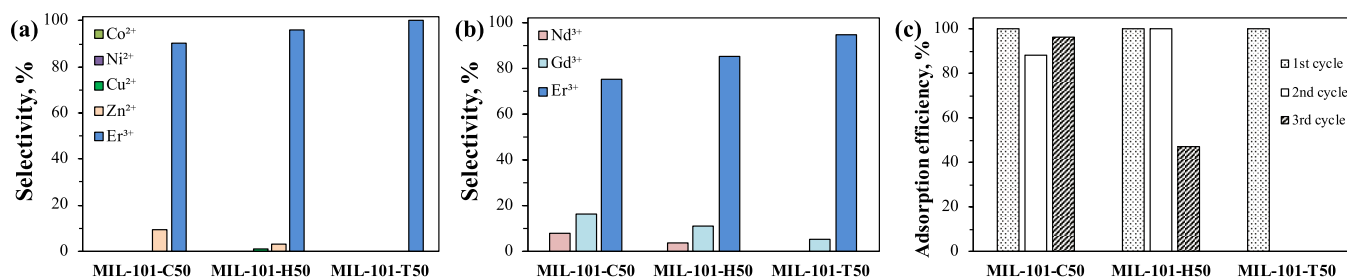


Fig. 4. Adsorption selectivity for Er^{3+} against transition (a) and rare earth metal ions (b) on the modified MIL-101 materials at pH 5.5, (c) adsorption–desorption cycles of the functionalized MIL-101.

Table 2

Adsorption capacities for Nd^{3+} , Gd^{3+} and Er^{3+} at concentration 200 ppm and distribution coefficients of modified samples.

Sample	q_e (mg g^{-1})			K_d (mL g^{-1})		
	Nd^{3+}	Gd^{3+}	Er^{3+}	Nd^{3+}	Gd^{3+}	Er^{3+}
MIL-101-C50	27.35	31.17	48.91	165	202	331
MIL-101-H50	34.86	44.91	57.47	221	321	421
MIL-101-T50	0.39	0	34.90	2	0	216

Table 3

Selectivity coefficients of adsorbents for heavy REEs in the presence of coexisting ions.

Adsorbent	$S_{X/REE}^a$	Reference
MIL-101-C50 (mixture of Nd^{3+} , Gd^{3+} and Er^{3+})	$\text{Er}^{3+}/\text{Nd}^{3+}$: 9.5 $\text{Er}^{3+}/\text{Gd}^{3+}$: 4.5	This work
MIL-101-H50 (mixture of Nd^{3+} , Gd^{3+} and Er^{3+})	$\text{Er}^{3+}/\text{Nd}^{3+}$: 22.8 $\text{Er}^{3+}/\text{Gd}^{3+}$: 7.7	This work
MIL-101-T50 (mixture of Nd^{3+} , Gd^{3+} and Er^{3+})	$\text{Er}^{3+}/\text{Nd}^{3+}$: n/ $\text{Er}^{3+}/\text{Gd}^{3+}$: 17.5	This work
U6N@ZIF-8-20 (mixture of Cd^{2+} , Zn^{2+} , Cu^{2+} , Mn^{2+} , Co^{2+} , Nd^{3+} , Eu^{3+} , Gd^{3+} and Er^{3+})	$\text{Er}^{3+}/\text{Nd}^{3+}$: 1.2 $\text{Er}^{3+}/\text{Gd}^{3+}$: 1.1	[21]
ZrP-0.71 (mixture of Cs^+ , Co^{2+} , Sr^{2+} , La^{3+} , Nd^{3+} , Eu^{3+} , Ho^{3+} and Yb^{3+})	no separation between REEs	[33]
ZrBTP-0.8 (mixture of Cs^+ , Co^{2+} , Sr^{2+} , La^{3+} , Ce^{3+} , Pr^{3+} , Nd^{3+} , Gd^{3+} , Dy^{3+} , Ho^{3+} and Th^{4+})	$\text{Ho}^{3+}/\text{Nd}^{3+}$: 3.2 $\text{Ho}^{3+}/\text{Gd}^{3+}$: 1.6	[35]
C4mim(8)@UiO-66 (mixture of La^{3+} , Nd^{3+} , Gd^{3+} and Yb^{3+})	$\text{Yb}^{3+}/\text{Nd}^{3+}$: 1.9 $\text{Yb}^{3+}/\text{Gd}^{3+}$: 1.4	[67]
0.075-AA-0.072@MIL-101 (mixture of Sc^{3+} , Y^{3+} and other REEs $^{3+}$)	$\text{Er}^{3+}/\text{Nd}^{3+}$: 1.0 $\text{Er}^{3+}/\text{Gd}^{3+}$: 1.1	[68]
PEI-CNC3 (mixture of Er^{3+} , La^{3+} , Eu^{3+})	$\text{Er}^{3+}/\text{La}^{3+}$: 2.9 $\text{Er}^{3+}/\text{Eu}^{3+}$: 3.2	[71]

^a $S_{X/REE} = q_{e,X}/q_{e,REE}$, where $q_{e,X}$ and $q_{e,REE}$ are the equilibrium capacity for a heavy rare earth element and corresponding REE, respectively.

^b No adsorption of Nd^{3+} .

remarkable selectivity (100%) without adsorption of any other bivalent metal ions. Further experimental work with a mixture of REEs revealed similar selectivity behaviour as for transition ions (Fig. 4b, Table 2). All

the materials had higher selectivity towards Er^{3+} than to Gd^{3+} and Nd^{3+} when compared to recently studied adsorbents (Table 3), such as MOFs [21,67–69], zirconium (IV) organophosphonates [33,35], commercial resins [70], PEI cellulose nanocrystals [71], and competitive with functionalized mesoporous silica KIT-6 [72]. Moreover, MIL-101-T50 shows practically no adsorption of Nd^{3+} or Gd^{3+} . Consequently, these adsorbents can be considered as potential candidates for separation of light and heavy REEs.

According to the hard-soft-acid-base (HSAB) theory [73], the functional groups of modifiers on the adsorbent surface are hard Lewis bases and an increase in their hardness is in the following order: Cyanex-272 < HDEHP < TBP [74–76]. The acidity of REEs decreases from heavy to light rare earth elements [77]. Taken together with the $\text{p}K_a$ values presented earlier (Section 3.2), these results may provide an explanation of the selectivity principle; namely, the softer the base group, the lower the selectivity for coordination with heavier REE ions, which is in line with the distribution and selectivity coefficients, presented in Tables 2 and 3, respectively.

3.6. Adsorption mechanism

The extraction process of REEs by phosphate esters, such as TBP, in acidic solutions is based on a solvation mechanism described by the following reaction [28,56]:

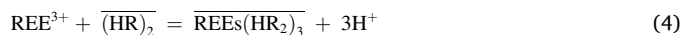


where the bar over TBP and its complex denote the presence of compounds in the organic phase.

In a recent study by Braatz et al. [78], it was shown that a charge-neutral complex with REEs can be formed with a lower number of TBP molecules, specifically 3 nitrate ions and 2 TBP molecules. Thus, the oxygen atom of the TBP molecule can be protonated by metalate anions, which results in complex formation between REE with three nitrate ions and two P=O groups of phosphate ester [28,56].

Comparison of the FTIR spectrum of MIL-101-T50 (Figure S11) before and after Er^{3+} adsorption shows a shift of the intense bands, respectively, from 1232 to 1121 cm^{-1} to 1178 and 1108 cm^{-1} . These shifts can indicate the complex formation with the rare earth ion through the P–O bond of the TBP compound [60,79]. Moreover, the decrease in intensity of the other peaks can be attributed to the previously noted leaching of TBP groups (Section 3.2) from the surface of MIL-101.

The utilization of phosphoric (HDEHP) and phosphinic (Cyanex-272) acids in the recovery of REEs is governed by ionic exchange or chelating mechanisms, represented by the following reaction [27,28,80,81]:



where HR represents the Cyanex-272 or HDEHP extractants. Based on the reaction, a charge-neutral complex with an extractant can be formed with six molecules of ligand for each metal ion [56,82].

After adsorption experiments, decreased intensities of bands at 1239, 1164 and 960 cm^{-1} for MIL-101-C50 were observed, indicating the coordination of Er^{3+} through P–O functional groups (Figure S1). Moreover, both shift and intensity enhancement of the original bands at 1143, 1071, and 1048 cm^{-1} to 1123, 1061 and 1042 cm^{-1} , respectively, can be ascribed to the coordination of phosphinic PO_2^- groups and Er^{3+} metal centres. In the case of MIL-101-H50, the FTIR spectra after Er^{3+} adsorption showed shifts from 1214 to 1161 cm^{-1} to 1178 and 1104 cm^{-1} , which can signify the involvement of P–O stretching and PO_2^- groups in complexation with the REE^{3+} [33,35]. Furthermore, the presence of new unique peaks at 485 and 483 cm^{-1} of the MIL-101-C50 and MIL-101-H50, respectively, can be assigned to the Er–O stretching vibration [30].

These results, together with the pH dependency and the extraction mechanisms [10], suggest that the most likely interaction between the Er^{3+} and functionalized MIL-101 can be interpreted as shown in Fig. 5. The functional groups of the materials at pH lower than 2 are highly protonated, causing the electrostatic repulsion of Er^{3+} ions and leading to low metal uptake. At higher pH, several phosphate P–O groups of MIL-101-T50 form coordinative complexes with adsorbate, which, as suggested by the data from TGA and adsorption isotherms, results in 4.6 molecules of modifier per each Er^{3+} ion. In addition, the functional groups of MIL-101-C50 and MIL-101-H50 are deprotonated at pH > 2 (i. e. $\text{pK}_a > 2$), providing strong coordinative affinity towards adsorbate by complexation through the P–O groups. Considering the loading of

MIL-101-H50, 3.4 modifier molecules are involved in adsorption of one Er^{3+} ion, which is nearly consistent with the discussion above.

3.7. Reusability

From the economic and environmental point of view, reusability of the adsorbent material is a crucial factor in any practical application. Adsorption experiments at different pH (Section 3.2) revealed the strong pH-dependency on the adsorption efficiency of Er^{3+} . Therefore, several adsorption–desorption experiments were conducted under acidic conditions [14,24,43] to evaluate the regeneration ability of the adsorbents (Fig. 4c).

As can be seen, the weakest performance by far is with MIL-101-T50, which demonstrated no adsorption of Er^{3+} after the first regeneration cycle. MIL-101-H50 maintained excellent adsorption capacity for two cycles, with reduced efficiency in the last run. Of the synthesized adsorbents, MIL-101-C50 demonstrated the best overall stability performance, and its adsorption efficiency remained around 96% at the end of the third cycle.

After three runs, XRD, SEM and FTIR analyses were utilized to appraise the stability of the materials (Figure S12, Figure S13 and Figure S14). XRD patterns and SEM images showed the intactness of the crystalline structures. However, as can be seen from Figure S14, the noted absence of characteristic peaks ascribed to P=O stretching (Section 3.1.5) of MIL-101-T50 can be attributed to substitution of the

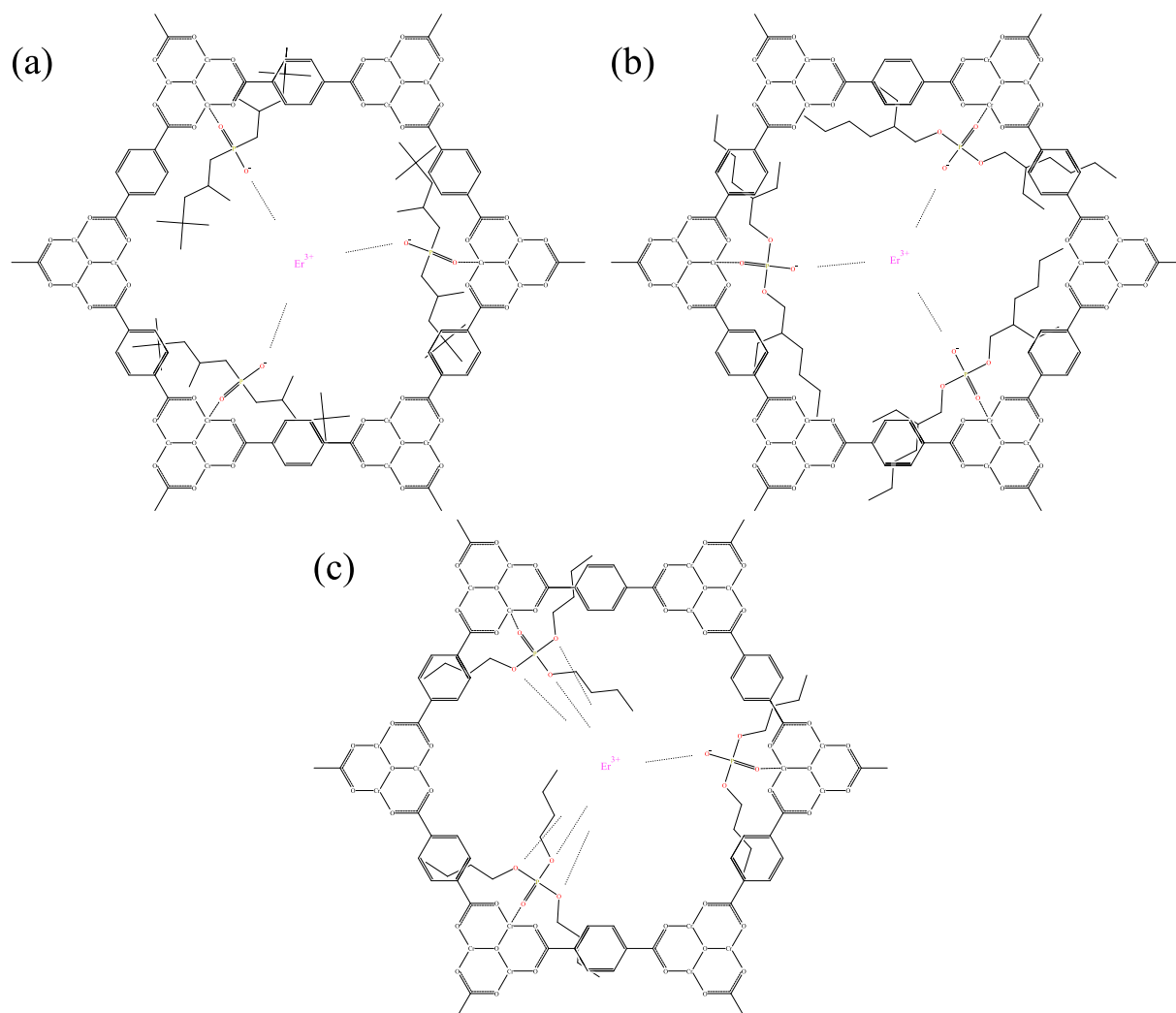


Fig. 5. Possible mechanism of adsorption of Er^{3+} by (a) MIL-101-C50, (b) MIL-101-H50 and (c) MIL-101-T50 (the nitrate anions presented around Er^{3+} have been omitted for clarity reasons).

functional groups by water molecules, as mentioned in Section 3.2. It should be noted that degradation of the TBP groups was not detected after adsorption experiments at pH 2 and pH 5.5 (Figure S6) and only found after the desorption cycle at much lower pH. The low stability correlates with results from ICP-MS (Table S4) showing the highest concentration of leached P after the adsorption experiments at acidic conditions (pH 1). High protonation of the groups in the desorption stage may cause disruption of the bonding between the functional groups and CUS of Cr(III) [24].

FTIR spectra of MIL-101-H50 and MIL-101-C50 showed no apparent loss of functional groups, suggesting that the reason for the decreased efficiency of MIL-101-H50 may be insufficient reaction time or acidity at desorption stage [83] for releasing of Er^{3+} from occupied adsorption sites. Nevertheless, MIL-101-H50 and MIL-101-C50 demonstrated good chemical stability during the adsorption–desorption cycles.

4. Conclusions

The aim of the current study was to determine the applicability and efficiency of MIL-101(Cr) post-synthetically modified with organophosphorus compounds for the selective recovery of REEs and potential separation of HREEs from LREEs in aqueous solutions.

MIL-101(Cr) was synthesized by the stoichiometric addition of 1:1 nitric acid:chromium nitrate and further functionalized with Cyanex-272, HDEHP and TBP. The presence of functional groups of modifiers and their successful grafting on the surface of MIL-101(Cr) were confirmed by observable changes in FTIR, BET and TGA analyses after modification. In general, study of the adsorption of Nd^{3+} , Gd^{3+} and Er^{3+} ions identified higher affinity of all functionalized materials towards heavier REEs. Maximum experimental adsorption capacities for Er^{3+} were achieved at optimal pH 5.5 for all synthesized adsorbents and found as 37.2, 48.9 and 57.5 mg g^{-1} for MIL-101-T50, MIL-101-C50 and MIL-101-H50, respectively. The adsorption isotherms and kinetic studies showed heterogeneity of the surface of the adsorbents and pointed to strong complex interaction with the adsorbate.

The present study appears to be the first report in which the selectivity of the functionalized metal-organic frameworks towards heavy REE over 90% against transition metal ions and more than 75% in a mixture of rare earth ions (Nd^{3+} , Gd^{3+} and Er^{3+}) was demonstrated. Moreover, the highest selectivity performance of 100% and 95% towards Er^{3+} against bivalent metals and REEs, respectively, was achieved by MIL-101-T50. Reusability study showed that MIL-101-C50 and MIL-101-H50 can preserve their structural and functional properties well for at least two cycles. The adsorption capability of MIL-101-T50 weakened greatly after the first cycle. The formation of coordinative complexes between the adsorbate and P–O groups of organophosphorus ligands on the surface of the modified MIL-101(Cr) can be suggested as a potential adsorption mechanism of Er^{3+} . Further research, together with computational modelling, could clarify further the complex formation mechanism. Moreover, linking by covalent bonds of TBP molecules with MOF structures could be investigated to enable synthesis of stable adsorbent with high selectivity towards heavy REEs. Future studies could also investigate the removal of uranium by MOFs modified with the organophosphorus compounds studied in this work.

Author contribution

Vitalii Kavun: Conceptualization, Methodology, Formal analysis, Investigation, Writing - Original Draft, Visualization. Monique A. van der Veen: Writing - Review & Editing, Supervision. Eveliina Repo: Conceptualization, Writing - Review & Editing, Supervision, Funding acquisition.

Declaration of competing interest

The authors declare that they have no known competing financial

interests or personal relationships that could have appeared to influence the work reported in this paper.

Acknowledgments

The authors are grateful for the valuable assistance of Dr. Liisa Puro, Toni Väkiparta and Esmaeili Mohammadamin. This work was supported by the Emil Aaltonen Foundation (Tampere, Finland).

Appendix A. Supplementary data

Supplementary data related to this article can be found at <https://doi.org/10.1016/j.micromeso.2020.110747>.

References

- [1] E.U. European Union. <https://doi.org/10.2873/11619>, 2020.
- [2] M. Sethurajan, E.D. van Hullebusch, D. Fontana, A. Akcil, H. Deveci, B. Batinic, J. P. Leal, T.A. Gasche, M. Ali Kucuker, K. Kuchta, I.F.F. Neto, H.M.V.M. Soares, A. Chmielarz, Crit. Rev. Environ. Sci. Technol. 49 (2019) 212–275, <https://doi.org/10.1080/10643389.2018.1540760>.
- [3] Think Tank Recovery of Rare Earths from Electronic Wastes: an Opportunity for High-Tech SMEs, 2015, 518777, 2015, http://www.europarl.europa.eu/thinktank/en/document.html?reference=IPOL_STU, accessed December 2019.
- [4] Y. Yang, A. Walton, R. Sheridan, K. Güth, R. Gauß, O. Gutfleisch, M. Buchert, B. M. Steenari, T. Van Gerven, P.T. Jones, K. Binnemans, J. Sustain. Metall. 3 (2017) 122–149, <https://doi.org/10.1007/s40831-016-0090-4>.
- [5] C.E.D. Cardoso, J.C. Almeida, C.B. Lopes, T. Trindade, C. Vale, E. Pereira, Nanomaterials 9 (2019) 814, <https://doi.org/10.3390/nano9060814>.
- [6] M. Gergoric, C. Ravaux, B.-M. Steenari, F. Espegren, T. Retegan, Metals 8 (2018) 721, <https://doi.org/10.3390/met8090721>.
- [7] A. Chagnes, G. Cote, C. Ekberg, M. Nilsson, T. Retegan (Eds.), Hydrometallurgical Processes for the Recovery of Metals from WEEE, Elsevier, 2016, pp. 139–175.
- [8] S. Wu, L. Wang, L. Zhao, P. Zhang, H. El-Shall, B. Moudgil, X. Huang, L. Zhang, Chem. Eng. J. 335 (2018) 774–800, <https://doi.org/10.1016/j.cej.2017.10.143>.
- [9] E.R. Rene, E. Sahinkaya, A. Lewis, P.N.L. Lens (Eds.), Leaching and Recovery of Metals, Springer, Cham, 2017, pp. 161–206.
- [10] F. Xie, T.A. Zhang, D. Dreisinger, F. Doyle, Miner. Eng. 56 (2014) 10–28, <https://doi.org/10.1016/j.mineng.2013.10.021>.
- [11] M.J. Page, K. Soldenhoff, M.D. Ogden, Hydrometallurgy 169 (2017) 275–281, <https://doi.org/10.1016/j.hydromet.2017.02.006>.
- [12] S.M. Abdelbasir, C.T. El-Sheltawy, D.M. Abdo, J. Sustain. Metall. 4 (2018) 295–311, <https://doi.org/10.1007/s40831-018-0175-3>.
- [13] I. Anastopoulos, A. Bhatnagar, E.C. Lima, J. Mol. Liq. 221 (2016) 954–962, <https://doi.org/10.1016/j.molliq.2016.06.076>.
- [14] T. Barcelos da Costa, M.G. Carlos da Silva, M.G. Adeodato Vieira, J. Rare Earths (2019), <https://doi.org/10.1016/j.jre.2019.06.001>.
- [15] A.J. Howarth, A.W. Peters, N.A. Vermeulen, T.C. Wang, J.T. Hupp, O.K. Farha, Chem. Mater. 29 (2017) 26–39, <https://doi.org/10.1021/acs.chemmater.6b02626>.
- [16] S. Yuan, L. Feng, K. Wang, J. Pang, M. Bosch, C. Lollar, Y. Sun, J. Qin, X. Yang, P. Zhang, Q. Wang, L. Zou, Y. Zhang, L. Zhang, Y. Fang, J. Li, H.-C. Zhou, 1704303, <https://doi.org/10.1002/adma.201704303>, 2018.
- [17] B.N. Bhadra, A. Vinu, C. Serre, S.H. Jung, Mater. Today 25 (2019) 88–111, <https://doi.org/10.1016/j.mattod.2018.10.016>.
- [18] R. Abazari, S. Sanati, A. Morsali, Chem. Commun. 56 (2020) 6652–6655, <https://doi.org/10.1039/D0CC01146K>.
- [19] P. Li, J.Z. Li, X. Feng, J. Li, Y.C. Hao, J.W. Zhang, H. Wang, A.X. Yin, J.W. Zhou, X. J. Ma, B. Wang, Nat. Commun. 10 (2019) 2177, <https://doi.org/10.1038/s41467-019-10218-9>.
- [20] R. Abazari, A. Morsali, D.P. Dubal, Inorg. Chem. Front. 7 (2020) 2287–2304, <https://doi.org/10.1039/D0QI00050G>.
- [21] M. Zhang, K. Yang, J. Cui, H. Yu, Y. Wang, W. Shan, Z. Lou, Y. Xiong, Chem. Eng. J. 386 (2020), 124023, <https://doi.org/10.1016/j.cej.2020.124023>.
- [22] D. Chen, W. Shen, S. Wu, C. Chen, X. Luo, L. Guo, Nanoscale 8 (2016) 7172–7179, <https://doi.org/10.1039/C6NR00695G>.
- [23] K. Leus, T. Bogaerts, J. De Decker, H. Depauw, K. Hendrickx, H. Vrielinck, V. van Speybroeck, P. van der Voort, Microporous Mesoporous Mater. 226 (2016) 110–116, <https://doi.org/10.1016/j.micromeso.2015.11.055>.
- [24] Y.-R. Lee, K. Yu, S. Ravi, W.-S. Ahn, ACS Appl. Mater. Interfaces 10 (2018) 23918–23927, <https://doi.org/10.1021/acsami.8b07130>.
- [25] S.A. Wood, Chem. Geol. 82 (1990) 159–186, [https://doi.org/10.1016/0009-2541\(90\)90080-Q](https://doi.org/10.1016/0009-2541(90)90080-Q).
- [26] J. Zhao, F. Huo, F. Pan, D. Li, H. Liu, Ind. Eng. Chem. Res. 53 (2014) 1598–1605, <https://doi.org/10.1021/ie403414j>.
- [27] J.E. Quinn, K.H. Soldenhoff, G.W. Stevens, N.A. Lengkeek, Hydrometallurgy 157 (2015) 298–305, <https://doi.org/10.1016/j.hydromet.2015.09.005>.
- [28] A. Ferdowsi, H. Yoozbashizadeh, Metall. Mater. Trans. B 48 (2017) 3380–3387, <https://doi.org/10.1007/s11663-017-1086-6>.
- [29] C. Basualto, J. Gaete, L. Molina, F. Valenzuela, C. Yañez, J.F. Marco, Sci. Technol. Adv. Mater. 16 (2015), 035010, <https://doi.org/10.1088/1468-6996/16/3/035010>.

- [30] M.S. Gasser, E. El Sherif, R.O. Abdel Rahman, *Chem. Eng. J.* 316 (2017) 758–769, <https://doi.org/10.1016/j.cej.2017.01.129>.
- [31] H. Zhou, D. Li, Y. Tian, Y. Chen, *Rare Met.* 27 (2008) 223–227, [https://doi.org/10.1016/S1001-0521\(08\)60119-9](https://doi.org/10.1016/S1001-0521(08)60119-9).
- [32] Q. Shu, A. Khayambashi, Q. Zou, X. Wang, Y. Wei, L. He, F. Tang, *J. Radioanal. Nucl. Chem.* 313 (2017) 29–37, <https://doi.org/10.1007/s10967-017-5293-z>.
- [33] J. Velisek-Carolan, T.L. Hanley, V. Luca, *Separ. Purif. Technol.* 129 (2014) 150–158, <https://doi.org/10.1016/j.seppur.2014.03.028>.
- [34] Q. Gao, J.F. Xie, Y.T. Shao, C. Chen, B. Han, K.S. Xia, C.G. Zhou, *Chem. Eng. J.* 313 (2017) 197–206, <https://doi.org/10.1016/j.cej.2016.12.068>.
- [35] V.V. Luca, J.J. Tejada, D. Vega, G. Arrachart, C. Rey, *Inorg. Chem.* 55 (2016) 7928–7943, <https://doi.org/10.1021/acs.inorgchem.6b00954>.
- [36] Y. Hu, J. Florek, D. Larivière, F.-G. Fontaine, F. Kleitz, *Chem. Rec.* 18 (2018) 1261–1276, <https://doi.org/10.1002/tcr.201800012>.
- [37] G. Férey, C. Mellot-Draznieks, C. Serre, F. Millange, J. Dutour, S. Surblé, I. Margiolaki, *Science* 309 (2005) 2040–2042, <https://doi.org/10.1126/science.1116275>.
- [38] D.-Y. Hong, Y.K. Hwang, C. Serre, G. Férey, J.-S. Chang, *Adv. Funct. Mater.* 19 (2009) 1537–1552, <https://doi.org/10.1002/adfm.200801130>.
- [39] Y.K. Hwang, D.-Y. Hong, J.-S. Chang, S.H. Jung, Y.-K. Seo, J. Kim, A. Vimont, M. Daturi, C. Serre, G. Férey, *Angew. Chem. Int. Ed.* 47 (2008) 4144–4148, <https://doi.org/10.1002/anie.200705998>.
- [40] M. Shafiei, M.S. Alivand, A. Rashidi, A. Samimi, D. Mohebbi-Kalhari, *Chem. Eng. J.* 341 (2018) 164–174, <https://doi.org/10.1016/j.cej.2018.02.027>.
- [41] J.N. Hall, P. Bollini, *React. Chem. Eng.* 4 (2019) 207–222, <https://doi.org/10.1039/c8re00228b>.
- [42] M. Sheikh Alivand, N.H.M. Hossein Tehrani, M. Shafiei-Alavijeh, A. Rashidi, M. Kooti, A. Pourreza, S. Fakhraie, *J. Environ. Chem. Eng.* 7 (2019), 102946, <https://doi.org/10.1016/j.jece.2019.102946>.
- [43] Z.Q. Bai, L.Y. Yuan, L. Zhu, Z.R. Liu, S.Q. Chu, L.R. Zheng, J. Zhang, Z.F. Chai, W. Q. Shi, *J. Mater. Chem.* 3 (2015) 525–534, <https://doi.org/10.1039/c4ta04878d>.
- [44] Z. Niu, W.D.C. Bhagya Gunatilleke, Q. Sun, P.C. Lan, J. Perman, J.G. Ma, Y. Cheng, B. Aguila, S. Ma, *Inside Chem.* 4 (2018) 2587–2599, <https://doi.org/10.1016/j.chempr.2018.08.018>.
- [45] T. Zhao, F. Jeremias, I. Boldog, B. Nguyen, S.K. Henninger, C. Janiak, *Dalton Trans.* 44 (2015) 16791–16801, <https://doi.org/10.1039/c5dt02625c>.
- [46] A. Buragohain, S. Couck, P. van der Voort, J.F.M. Denayer, S. Biswas, *J. Solid State Chem.* 238 (2016) 195–202, <https://doi.org/10.1016/j.jssc.2016.03.034>.
- [47] K.S.W. Sing, D.H. Everett, R.A.W. Haul, L. Moscou, R.A. Pierotti, J. Rouquerol, T. Siemieniowska, *Pure Appl. Chem.* 57 (1985) 603–619, <https://doi.org/10.1351/pac198557040603>.
- [48] M. Kruk, M. Jaroniec, R. Ryoo, S.H. Joo, *Chem. Mater.* 12 (2000) 1414–1421, <https://doi.org/10.1021/cm990764h>.
- [49] X.-J. Zhang, T.-Y. Ma, Z.-Y. Yuan, *Eur. J. Inorg. Chem.* (2008) 2721–2726, <https://doi.org/10.1002/ejic.200701368>, 2008.
- [50] S. van Rosendaal, B. Onghena, J. Roosen, B. Michielsen, K. Wyns, S. Mullens, K. Binnemans, *RSC Adv.* 9 (2019) 18734–18746, <https://doi.org/10.1039/c9ra02344e>.
- [51] Q. Shu, A. Khayambashi, X. Wang, Y. Wei, *Adsorpt. Sci. Technol.* 36 (2018) 1049–1065, <https://doi.org/10.1177/02663617417748112>.
- [52] M. Kouraim, N. Farag, S. Sadeak, M. Gado, *Int. J. Chem. Stud.* 2 (2014) 10–19.
- [53] C. Queffelec, M. Petit, P. Janvier, D.A. Knight, B. Bujoli, *Chem. Rev.* 112 (2012) 3777–3807, <https://doi.org/10.1021/cr2004212>.
- [54] T. Hatanaka, A. Matsugami, T. Nonaka, H. Takagi, F. Hayashi, T. Tani, N. Ishida, *Nat. Commun.* 8 (2017) 15670, <https://doi.org/10.1038/ncomms15670>.
- [55] T. Makanyire, S. Sanchez-Segado, A. Jha, *Adv. Manuf.* 4 (2016) 33–46, <https://doi.org/10.1007/s40436-015-0132-3>.
- [56] A.M. Wilson, P.J. Bailey, P.A. Tasker, J.R. Turkington, R.A. Grant, J.B. Love, *Chem. Soc. Rev.* 43 (2014) 123–134, <https://doi.org/10.1039/c3cs60275c>.
- [57] X. Fu, Z. Hu, Y. Liu, J.A. Golding, *Solvent Extr. Ion Exch.* 8 (1990) 573–595, <https://doi.org/10.1080/07366299008918018>.
- [58] K. Omelchuk, P. Szczepański, A. Shrotré, M. Haddad, A. Chagnes, *RSC Adv.* 7 (2017) 5660–5668, <https://doi.org/10.1039/c6ra21695a>.
- [59] K. Omelchuk, M. Stambouli, A. Chagnes, *J. Mol. Liq.* 262 (2018) 111–118, <https://doi.org/10.1016/j.molliq.2018.04.082>.
- [60] S. Mishra, J. Dwivedi, A. Kumar, N. Sankararamakrishnan, *New J. Chem.* 40 (2016) 1213–1221, <https://doi.org/10.1039/c5nj02639c>.
- [61] J. De Decker, K. Folens, J. De Clercq, M. Meledina, G. Van Tendeloo, G. Du Laing, P. van der Voort, *J. Hazard Mater.* 335 (2017) 1–9, <https://doi.org/10.1016/j.jhazmat.2017.04.029>.
- [62] V.G. Lade, P.C. Wankhede, V.K. Rathod, *Int. J. Chem. React. Eng.* 15 (2017) 83–91, <https://doi.org/10.1515/ijcre-2016-0035>.
- [63] R. Sips, *J. Chem. Phys.* 16 (1948) 490–495, <https://doi.org/10.1063/1.1746922>.
- [64] S.K. Papageorgiou, F.K. Katsaros, E.P. Kouvelos, N.K. Kanellopoulos, *J. Hazard Mater.* 162 (2009) 1347–1354, <https://doi.org/10.1016/j.jhazmat.2008.06.022>.
- [65] N. Ayawei, A.N. Ebelegi, D. Wankasi, *J. Chem.* 2017 (2017), 3039817, <https://doi.org/10.1155/2017/3039817>.
- [66] S. Sen Gupta, K.G. Bhattacharyya, *Adv. Colloid Interface Sci.* 162 (2011) 39–58, <https://doi.org/10.1016/j.cis.2010.12.004>.
- [67] I. Ahmed, K.K. Adhikary, Y.R. Lee, K. Ho Row, K.K. Kang, W.S. Ahn, *Chem. Eng. J.* 370 (2019) 792–799, <https://doi.org/10.1016/j.cej.2019.03.265>.
- [68] Z. Lou, X. Xiao, M. Huang, Y. Wang, Z. Xing, Y. Xiong, *ACS Appl. Mater. Interfaces* 11 (2019) 11772–11781, <https://doi.org/10.1021/acsami.9b00476>.
- [69] A.F. Abdel-Magied, H.N. Abdelhamid, R.M. Ashour, X. Zou, K. Forsberg, *Microporous Mesoporous Mater.* 278 (2019) 175–184, <https://doi.org/10.1016/j.micromeso.2018.11.022>.
- [70] X. Hérés, V. Blet, P. Di Natale, A. Ouattou, H. Mazouz, D. Dhba, F. Cueur, *Metals* 8 (2018) 682, <https://doi.org/10.3390/met8090682>.
- [71] F. Zhao, E. Repo, Y. Song, D. Yin, S. Ben Hammouda, L. Chen, S. Kalliola, J. Tang, K.C. Tam, M. Sillanpää, *Green Chem.* 19 (2017) 4816–4828, <https://doi.org/10.1039/c7gc01770g>.
- [72] Y. Hu, E. Drouin, D. Larivière, F. Kleitz, F.-G. Fontaine, *ACS Appl. Mater. Interfaces* 9 (2017) 38584–38593, <https://doi.org/10.1021/acsami.7b12589>.
- [73] R.G. Pearson, *J. Am. Chem. Soc.* 85 (1963) 3533–3539, <https://doi.org/10.1021/ja00905a001>.
- [74] P.K. Verma, P.K. Mohapatra, A. Bhattacharyya, A.K. Yadav, S.N. Jha, D. Bhattacharyya, *New J. Chem.* 42 (2018) 5243–5255, <https://doi.org/10.1039/c7nj04460g>.
- [75] W. Zhang, D. Avdibegović, R. Koivula, T. Hatanpää, S. Hietala, M. Regadio, K. Binnemans, R. Harjula, *J. Mater. Chem.* 5 (2017) 23805–23814, <https://doi.org/10.1039/c7ta08127h>.
- [76] C. Basualto, F. Valenzuela, L. Molina, J.P. Muñoz, E. Fuentesand, J. Sapag, *J. Chil. Chem. Soc.* 58 (2013) 1785–1789, <https://doi.org/10.4067/S0717-97072013000200032>.
- [77] V.S. Sastri, J.-C. Bünzli, V.R. Rao, G.V.S. Rayudu, J.R. Perumareddi, *Kinetics and Mechanisms of Rare Earth Complexation*, Elsevier, 2003, pp. 481–567.
- [78] A.D. Braatz, M.R. Antonio, M. Nilsson, *Dalton Trans.* 46 (2017) 1194–1206, <https://doi.org/10.1039/c6dt04305d>.
- [79] M. Alibrahim, H. Shleweit, *Period. Polytech. - Chem. Eng.* 51 (2007) 57–60, <https://doi.org/10.3311/pp.ch.2007-2.09>.
- [80] M. Nilsson, K.L. Nash, *Solvent Extr. Ion Exch.* 25 (2007) 665–701, <https://doi.org/10.1080/07366290701634636>.
- [81] J. Luo, C. Wang, J. Lan, Q. Wu, Y. Zhao, Z. Chai, C. Nie, W. Shi, *Sci. China Chem.* 59 (2016) 324–331, <https://doi.org/10.1007/s11426-015-5489-4>.
- [82] J.A. McCleverty, T.J. Meyer (Eds.), *Metal Complexes for Hydrometallurgy and Extraction*, Elsevier, 2004, pp. 759–808.
- [83] A. Battsengel, A. Batnasan, K. Haga, A. Shibayama, *J. Miner. Mater. Char. Eng.* 6 (2018) 517–530, <https://doi.org/10.4236/jmmce.2018.65037>.